Biointerface Research in Applied Chemistry
Open-Access Journal (ISSN: 2069-5837)

Article
Volume 13, Issue 2, 2023, 112
https://doi.org/10.33263/BRIAC132.112

Phyto-Decoration of Selenium Nanoparticles Using *Moringa peregrina* (Forssk.) Fiori Aqueous Extract: Chemical Characterization and Bioactivity Evaluation

Samer Y. Al-Qaraleh [1,*], Wael A. Al-Zereini [2], Sawsan A. Oran [1]

[1] Department of Biological Sciences, Faculty of Science, The University of Jordan, Amman 11942, Jordan
[2] Department of Biological Sciences, Faculty of Science, Mutah University, Al-Karak 61710, Jordan
* Correspondence: 75garalleh@gmail.com;

Scopus Author ID 56825949500
Received: 6.12.2021; Accepted: 10.01.2022; Published: 24.03.2022

Abstract: Selenium is an important trace element as a part of the seleno-proteins, which regulate the oxidative status of the body and is required for the normal physiological reaction. Biogenic synthesis of selenium nanoparticles (SeNPs) using plant extracts is recommended over microorganisms or chemical reactions. Herein, SeNPs were synthesized using *Moringa peregrina* leaves extract (MPM-SeNPs). The purified nanoparticles were chemically characterized by Fourier transform infrared (FT-IR), X-ray diffraction (XRD), scanning electron microscopy (SEM), dynamic light scattering (DLS), and energy-dispersive X-ray (EDX) analyses. The biological activity of MPM-SeNPs was evaluated by testing their antibacterial and antioxidant activities. Their anti-proliferative effect against breast cancer and normal fibroblast cell lines was also investigated. The highest absorption of biogenic MPM-SeNPs is 279 nm, and FT-IR analysis indicated peaks shifting and bending according to phenols, polysaccharides, and protein moieties. The Se-element made up 73.2 percent of the nanoparticles sample; they are agglomerated spheres with smooth surfaces and negative electric charges on their surfaces, with a diameter range of 80-150 nm. MPM-SeNPs revealed antibacterial activity against Gram-positive bacteria with MIC values of 20-50 µg/mL and radical scavenging potential at IC_{50} 23.6±0.2 µg/mL and 25.6±1.7 µg/mL in DPPH and ABTS assays, respectively. Moreover, the nanoparticles exhibited cytotoxic activity against breast cancer cell lines with an IC_{50} value of 129.4±4.4 µg/mL. MPM-SeNPs might have a potential role in the green synthesis of chemotherapeutic drugs and could be used as a natural agent in the food and pharmaceutical industries.

Keywords: anti-proliferative activity; antibacterial activity; antioxidant activity; *Moringa peregrina*; selenium nanoparticles.

1. Introduction

The burden of infectious diseases, cancer, and inflammatory disorders on human life increased in recent years. There is an upsurge in antibiotic resistance among various microbes, evolving of multidrug-resistant cancer cells, and escalation in the number of oxidative stress-associated diseases such as diabetes, asthma, arthritis, neuro-degradative, and other cellular deteriorations. Moreover, using chemotherapy and synthetic drugs is associated with hazardous effects on human health [1].

Application of nano- and biotechnology-based techniques in medical research led to preparations of nanomaterials dedicated to treating, diagnosis, control, and modulation of

biological systems [2]. Selenium (Se) is a chalcogen element that presents in various forms; selenide, selenate, and selenite [3]. It gains an important rank in the field of nanomedicine as a trace element required for normal physiochemical bioprocesses in the living cells [4] as well as part of selenoproteins; Se-containing enzymes such as thioredoxin reductase, glutathione peroxidase, and deiodinase that are involved in metabolic, activates antioxidant defense, and detoxification, respectively [5]. Se-deficiency might cause cancer, immune system imbalance, neurological dysfunction, and cognitive performance [1,6]. Se-nanoparticles (SeNPs) reveal biocompatibility, bio-efficacy, and lower toxicity [7]; it is widely accepted as a food supplement and in medicine as an antimicrobial, antioxidant, anti-inflammatory, antitumor, and drug delivery system [8].

The principal methods used in synthesizing SeNPs involve chemical, physical, and biological approaches [3]. Both chemical and physical ways are expensive, environmentally un-favorable, and toxic chemicals were used as reductants [9]; these methods require the usage of stabilizing agents that might be chemically toxic and hinder the compatibility of resulting NPs for biological applications. However, using plant extracts and microorganisms as bio-factories for SeNPs production is an eco-friendly and safe technique [10]. Captivatingly, using plant extracts is more expedient than microorganisms to evade the special conditions required to cultivate and maintain the microbial. Plant extracts provide agents that act as reductants and stabilizers; phenols, alkaloids, tannins, flavonoids, and saponins, among others, are examples of such reagents [11].

The genus Moringa includes 13 species that are distributed in several tropical and subtropical regions of the world [12]. They embrace compounds with high nutritional and medical values; flavonoids, phenolic acid, vitamins, minerals, and antioxidant compounds. The wonder plant *Moringa oleifera* Lam. was the most studied species among others; extracts from its different parts (pod, leave, seeds) possess antidiabetic, antipyretic, diuretic, antispasmodic, antihypertensive, cholesterol-lowering, antiulcer, anti-inflammatory, antitumor, hepatoprotective, antioxidant, and antimicrobial activities [13]. Some extracts were used to synthesize Ag, Zn, and Au nanoparticles with broad antimicrobial and anticancer potentials [14-16]. However, the biological importance of *M. peregrina* (Forssk.) Fiori was rarely addressed previously; in the past last 5 years, it gained the focus of researchers due to its value in traditional medicine. It is used to treat convulsions or infantile paralysis, asthma, hyperlipidemia, and hyperglycemia, antioxidant, wound healing, diabetes, constipation, muscle and back pains, headache, antitumor, and antimicrobial; these activities were attributed to the polyphenol, flavonoid, isothiocyanate, glycoside, and triterpenoid contents of the plant parts [17]. We know that extracts from different parts of *M. peregrina* have never been manipulated to produce elemental nanoparticles. Therefore, the current study addressed the green synthesis and characterization of SeNPs using aqueous extract of *M. peregrina* leaves with evaluating their antibacterial, antioxidant, and cytotoxic activities.

2. Materials and Methods

2.1. Plant collection and extraction.

The plant *M. peregrina* (Forssk.) Fiori (Family Moringacae, Order Brassicales) was collected from Wadi Bin-Hammad Valley/ Al-Karak Governorate, South of Jordan (31°18'03.0"N 35°37'34.9"E, GPS 31.300829, 35.626347). A voucher specimen was deposited at the Herbarium in the Department of Biology/Mutah University. It was identified and

authenticated by Prof. Sawsan Oran, Department of the Biological Sciences/University of Jordan. The plant leaves were cleaned up, dried in the shade, and ground to a fine powder. 50 g of pulverized material were soaked in 500 mL sterile distilled water and placed on a hotplate at 60°C with stirring for 15-30 min. The mixture was allowed to cool at ambient temperature before being filtered through filter paper (Whatman no.1) (Macherey-Nagel, Germany) and centrifuged for 5 minutes at 1500 rpm (Combi-514R, Korea). The aqueous extract that resulted was kept at 4°C until it was used.

2.2. Qualitative phytochemical screening.

The main constituent of *M. peregrina* aqueous extract was preliminarily identified using thin-layer chromatography (TLC, 20 × 20 cm, Macherey & Nagel, Germany) following previous procedures [18]. The developed spots were visualized under UV (254 and 366 nm); the presence of flavonoids was detected by spraying with an ethanolic solution of aluminum chloride; phenols, terpenes, sugars, and terpenes were identified by using *p*-anisaldehyde/sulfuric acid solution, and Dragendroff's reagent revealed the presence of alkaloids.

2.3. Quantitative phytochemical analysis.

Quantitative analyses of total phenol (TPC), flavonoid (TFC), and tannin (TTC) contents were performed following methods reported previously [10]. TPC and TTC were determined using Folin–Ciocalteu's reagent against standard curves of gallic acid at 765 nm and tannic acid at 720 nm; the contents were expressed as gallic acid equivalents (mg GAE/g of plant extract) and tannic acid equivalent (mg TAE/g of plant extract), respectively. While TFC was determined by the aluminum chloride colorimetric method against the rutin standard curve at 520 nm, the content was expressed as rutin equivalents (mg RE/g of plant extract). All quantification experiments were performed in triplicates, and results are expressed as mean values ± standard deviation (SD).

2.4. Se-nanoparticles synthesis and characterization.

Synthesis of SeNPs was achieved using 10 mM sodium selenite solution (Na_2SeO_3, BDH chemicals, UK) as a precursor following a previous procedure [10], with some modifications. Briefly, definite volumes of aqueous leaves extract (2, 4, 6, 8, 10 mL) were added dropwise to 10 mL of 10 mM Na_2SeO_3 with magnetic stirring. The optimized condition for nanoparticles synthesis was noticed when 4 mL leaves extract was added to 10 mL of 10 mM precursor solution, which was kept at room temperature. The reduction of Na_2SeO_3 to nano-selenium was carried out in the dark for 24 hours at 37±2°C, and at 150 rpm agitation speed. The formation of *M. peregrina* mediated SeNPs (MPM-SeNPs) was evident by changing mixture color from pale yellow into brick-red solution. The nanoparticle formation and color intensity change were followed using UV/Vis spectrophotometer Hitachi U-5100 (Hitachi, Japan) with scanning protocol from 200-800 nm. The formed MPM-SeNPs were collected by centrifugation at 15000 g for 30 min (Hermle, Germany), washed three times with deionized water followed by ethanol, and dried overnight. A suspension of nanoparticles was prepared in sterile phosphate buffer (pH 7.4) and stored at 4°C until further analysis and experiments.

For the characterization of MPM-SeNPs, the absorption spectrum was deduced using UV/Vis spectrophotometer Hitachi U-5100 (Hitachi, Japan). The absorbance was scanned at wavelength range 200-800 nm with 1 nm wavelength intervals and 1 cm path length. The presence of various functional groups fabricating the surface of MPM-SeNPs was detected using Fourier transform infrared (FT-IR) spectrometer (Bruker, USA), spectra were acquired at 400–4000 cm^{-1} wavenumbers against potassium bromide background. The surface structure and crystalline form of the nanoparticles were detected by X-ray diffraction technique (XRD) using Rigaku Ultima IV X-ray diffractometer (Rigaku, Japan) operated at 40 kV/20 mA with CuKα radiation (λ = 1.5405 Å) over a scanning range of Bragg angles (2θ) from 20° to 80°. The average size of the crystallized nanomaterial was calculated using the Scherrer equation:

$$D= k\lambda/\beta\cos\theta$$

where D is the crystal size, λ is the applied X-ray wavelength (1.54 Å), k is the numerical constant with a value of 0.94, β½ is the full width (radians) at half maximum of the signal (FWHM) in 2θ value [19].

The morphology of the phyto-synthesized MPM-SeNPs was elucidated using Quanta 450 FEG scanning electron microscopy (SEM) (FEI Company, USA). The nanoparticle suspension was dried, loaded on the sample holder, coated with gold in a vacuum, and images of different magnifications were taken at 30 kV. Meanwhile, the amount of selenium element in the nanoparticles was deduced using dispersive X-ray spectroscopy (EDX) at 20 kV (EDX-7000, Shimadzu, Japan). The hydrodynamic size distribution and zeta potential of the MPM-SeNPs were monitored at 25°C by dynamic light scattering method (DLS) using the Malvern Zetasizer (Nano ZS Malvern, UK).

2.5. Biological activity evaluation.

2.5.1. Antibacterial activity.

The antibacterial activity of the MPM-SeNPs was determined by a well diffusion test, and the minimum inhibitory concentration (MIC) was determined by micro-broth dilution assay according to Clinical and Laboratory Standards Institute guidelines and as described previously [20], with some modifications. Tested bacterial strains were the Gram-negative bacteria [*Pseudomonas aeruginosa* (ATCC 13048) and *Escherichia coli* (ATCC 25922)] and the Gram-positive bacteria [*Staphylococcus aureus* (ATCC 43300), *Bacillus cereus* (ATCC 11778), and *B. subtilis* (ATCC 6633)]. Wells of 6 mm diameters were made using a sterile Cork borer in Muller Hinton agar plates seeded with an overnight culture of tested bacteria at cell density 10^6 cell/mL. To each well in the bacterial agar plates, 100 µl aliquots were added from either MPM-SeNPs preparation (20 µg/well), 10 mM Na_2SeO_3 (173 µg/well), or aqueous plant extract (2 mg/well). Streptomycin (10 µg/disc, Bio Basic Inc, Canada) was used as a positive control, and the results are presented as means of three independent tests ± SD.

However, in the micro-broth dilution assay, MPM-SeNPs and the positive control were tested starting from 100 µg/mL and 50 µg/mL, respectively. Type of inhibition, bactericidal or bacteriostatic, was determined by platting the preparations in micro-broth dilution assay, where there were no visible growths, on agar plates with proper medium and incubation for 24 h.

2.5.2. Antioxidant activity.

The ability of synthesized nanoparticles, Na_2SeO_3, and plant extract to neutralize and decolorize 1,1-diphenyl-2-picrylhydrazyl (DPPH, Sigma-Aldrich, Germany) or 2,2'-Azino-bis-(3-ethyl-benzothiazoline-6-sulfonic acid) (ABTS, Sigma-Aldrich, Germany) radicals were examined as an indication of their antioxidant potential [21]. Briefly, 10 µl of different concentrations of MPM-SeNPs, plant extract, or Na_2SeO_3 were added to 1 mL methanolic solution of 0.1 mM DPPH. The preparation was mixed thoroughly and incubated at 37°C for 20 min. The decrease in the starting absorbance of the resulting solution, OD_{517nm} 0.7-0.8, was measured at 517 nm by UV/Vis spectrophotometer Hitachi U-5100 (Hitachi, Japan). In ABTS assay, 7 mM ABTS and 2.45 mM potassium persulfate were reacted together, final concentrations in distilled water, and incubated at room temperature in darkness for 16 h to generate $ABTS^{\bullet+}$ radical cation. The generated radical solution was diluted to an absorbance of 0.700 ± 0.005 at 734 nm UV/Vis Spectrophotometer using ethanol. To 2 mL of diluted $ABTS^{\bullet+}$, 10 µl of different concentrations from test samples was added and mixed vigorously. The reactive mixture was allowed to stand at room temperature for 6 min, and the absorbance was recorded immediately at 734 nm. The scavenging activity of tested substances in the neutralization of DPPH or $ABTS^{\bullet+}$ radicals was calculated according to the formula

$$\text{Scavenging effect (\%)} = [(A_{control} - A_{sample})/ A_{control}] \times 100$$

Methanol (99.9%) was used as a blank, and Trolox standard (concentrations from 0 to 1.5 µg/mL) in ethanol was prepared and assayed using the same conditions. All results are expressed in terms of the mean value of Trolox® equivalent antioxidant capacity (TEAC). The assay was performed in triplicate for each sample and each standard concentration. The concentration required to inhibit 50% of formed radicals (IC_{50}) was interpolated from a dose-response curve plotted for percentage inhibitions against respective concentrations of each tested material.

2.5.3. Cytotoxic activity

The effect of aqueous plant extract, MPM-SeNPs, and Na_2SeO_3 on the proliferation of the human dermal fibroblast (ATCC® PCS-201-012) and breast cancer adenocarcinoma MDA-MB-231 (ATCC® HTB-26) cell lines was evaluated as described previously [22]. The cells were cultured in Dulbecco's Modified Eagle Medium (DMEM; Gibco, Germany) supplemented with L-glutamine, 10% heat-inactivated fetal calf serum (Gibco, Germany), 65 µg/mL of penicillin G, and 100 µg/mL of streptomycin sulfate. They were kept at 37°C in a humidified environment with 5.0% CO_2. Different concentrations of tested materials (1-200 µg/mL) were administrated to wells containing 0.5–1×10^5 cell/mL. The cytotoxic effect was observed microscopically as well as quantitatively by using Giemsa stain after 72 h. The data were expressed as mean ± SD of three independent experiments. The concentration required to inhibit 50% of cell proliferation (IC_{50}) was interpolated from a dose-response curve plotted for percentage inhibitions against respective substance concentrations.

2.6. Selectivity index

The selectivity index is the ratio for sample or drug cytotoxicity against normal dermal fibroblast cells to its cytotoxicity against cancer cells. Values greater than 1 indicate that sample

has selective activity against cancer compared to non-cancer cells *in vitro*. It was calculated according to the formula:

$$\text{Selectivity index (SI)} = IC_{50}^{\text{normal fibroblast cells}} / IC_{50}^{\text{cancer cells}}$$

2.7. Statistical analysis.

All results are reported as mean ± standard deviation (SD). The dose-response curve was determined using PROBIT regression analysis with a 95% confidence limit [23]. Results were analyzed by one-way ANOVA and Tukey HSD *post hoc* test using the Statistical Package for the Social Sciences software (SPSS, version 16). Data were considered significant at $p<0.05$.

3. Results and Discussion

Plants draw the interest of scientific and pharmaceutical communities as eco-friendly, high nutritional, and complementary medicinal sources for bioactive secondary metabolites; they were appraised as prodigious antioxidants, antimicrobial, and anticancer agents. Interestingly, plant metabolites were reported as candidates for the green synthesis of biologically active nanoparticles; they act as reducing and stabilizing agents. *M. oleifera* extracts were extensively studied as biologically active agents and bio-synthesizers for nanoparticles with pharmaceutical potentials [13-16]; however, no studies on using M. peregrina extracts to manufacture nano-elements.

3.1. Chemical analysis of M. peregrina aqueous extract.

The total contents of major classes of secondary metabolites in *M. peregrina* extract were quantitatively determined to link their amount with the reducing ability of the plant extract in synthesizing SeNPs. In the current study, an aqueous extract of *M. peregrina* embraced phenols, flavonoids, terpenes, glycosides, and steroids detected using TLC. Quantitatively, TPC in the plant extract was 169.8±0.53 mg GAE/g of plant extract; TFC and TTC were 20.2±0.87 mg RE/g of plant extract and 88±0.98 mg TAE/g of plant extract, respectively. The qualitative analysis of the main chemical constituents of *M. peregrina* aqueous extract documented herein coincided with those detected in the ethanolic extract [24] and literate isolated chemicals from different parts of the same species [17], as well as with those reported in ethanolic extract of *M. oleifera* [25]. However, the herein determined TPC in *M. peregrina* extract was relatively analogous to that reported by Hamed *et al*. [26] (142.85 mg GAE/g plant extract) but slightly higher than that reported in previous studies on aqueous plant extract [27] and on different organic extracts which ranged from 53.4-137.53 mg GAE/g extract [24,28,29]. Eventually, the TPC of *M. peregrina* aqueous extract was more than those reported in other Moringa species [25,29,31].

Meanwhile, the reported TFC of aqueous plant leaves extract was within the documented amounts in aqueous, ethanolic, and methanolic extracts from *M. peregrina* and other Moringa species, which were 9.59-57 mg quercetin equivalent (QE)/g crude extract [24,29,30]; worth noting, some reports revealed much higher flavonoid content in methanolic extract of *M. oleifera* compared to other extract types [30,31]. Remarkably, variation between reported TPC and TFC between Moringa species and even within the same species might be

attributed to several factors, including experiment techniques, country of cultivation, weather conditions, type of soils, time of collections, and type of extractants [32].

3.2. Biosynthesis and characterization of MPM-SeNPs.

The synthesis of MPM-SeNPs was successfully achieved using the aqueous extract of *M. peregrina*; bioreduction of the Na_2SeO_3 solution to the Se^0 element by plant extract was confirmed by the color change of reaction mixture from colorless (precursor) to brick red solution (Figure 1A, the inset) with maximum absorption (λmax) between 260-350 nm and the highest peak at 279 nm due to the Surface Plasmon Resonance (SPR) of the formed nanoparticles (Figure 1A). During the optimization process of MPM-SeNPs production, periodic sampling of the reaction mixture indicated an increase in the UV/Vis spectrum by the increase of reaction time up to 24 h and plant extract concentration (Figure 1B); nanoparticles prepared at plant concentrations > 4 mL plant extract in 10 mL of 10 mM Na_2SeO_3 (v/v) were unstable and precipitated (agglomerated) within 3 days of storage at 4°C. Thus, adding 4 mL leaves' aqueous extract to 10 mL of 10 mM precursor solution with 24 h reaction time was adopted as an optimized condition for nanoparticle synthesis. The current depicted maximum absorption coincided with the reported λmax of SeNPs biosynthesized using several plant extracts [10,33,34] and microorganisms [5,35,36] 200-400 nm, indicating the role of their metabolites in stabilizing and reducing the precursor salt.

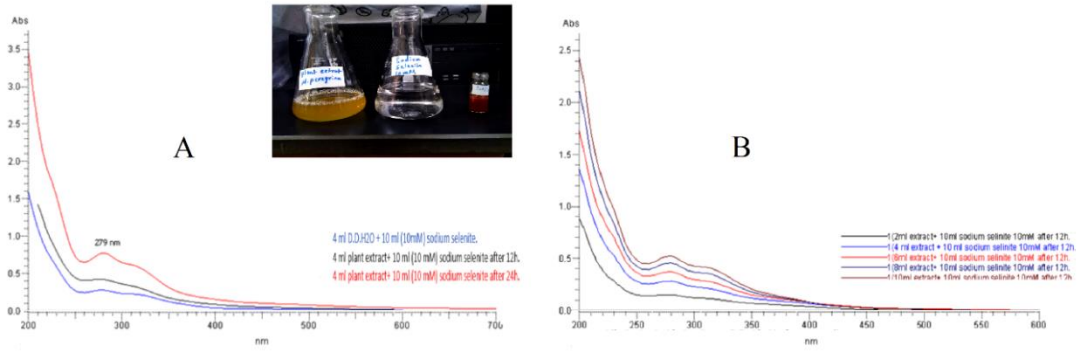

Figure 1. UV-visible spectra of phyto-synthesized MPM-SENPs showing an increase in absorbance intensity of reaction mixture at 0, 12, and 24 h time intervals. (**A**) increase in the intensity of maximum absorbance peak of MPM-SeNPs development (inset) due to the Surface Plasmon Resonance, (**B**) effect of an increase in plant extract concentration on the intensity of UV/Vis spectrum intensity of MPM-SeNPs.

FT-IR analysis unveil the spectra of biomolecules responsible for synthesizing and stabilizing MPM-SeNP (Figure 2). It revealed dominant peaks in *M. peregrina* aqueous extract at wavenumbers 3380.24 cm^{-1}, 1612.46 cm^{-1}, and 1099.77 cm^{-1} corresponding to OH- a vibrational stretch of alcohol and phenol [10], amide I vibration or might be C=O and C-H stretching of flavonoid structures [5, 33], and C-O-C as well as C-O polysaccharide vibration [37], respectively. Additionally, small peaks at 2936.03 cm^{-1}, 1514.06 cm-1, 1441.5 cm^{-1}, and 600.49 cm^{-1} were assigned to C-H stretching in alkynes [10,38], N-H bending of amide II [37], asymmetric C-H bending vibration [38], and phenolic O-H bending vibration [10], respectively. Interestingly, vibrational bands 3380.24 cm^{-1}, 2936.03 cm^{-1}, and 1099.77 cm^{-1} were shifted to 3427.18 cm^{-1}, 2918.91 cm^{-1}, and 1095.07 cm^{-1} in synthesized MPM-SeNPs respectively. Moreover, the peak at wavenumber 1612.46 cm-1 in plant extract was split into two stretching vibrations at 1629.77 cm^{-1} and 1640.49 cm^{-1}, while new peaks appeared in the nanoparticle's spectrum at 2309.91 (C-H bending), 1322 (C-H stretching), and 766.75 (C-H

bending out of aromatic plane); all peaks shifting and unveiling of new ones indicated interaction of phenols, polysaccharide, and protein contents of *M. peregrina* extract in bioreduction and synthesis of MPM-SeNPs.

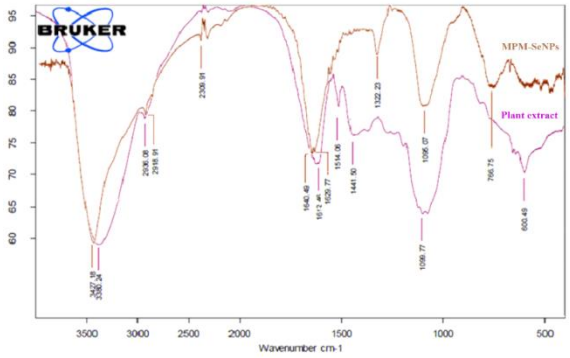

Figure 2. FT-IR spectra of phyto-synthesized MPM-SeNPs and plant aqueous extract.

The crystalline structure of *M. peregrina* mediated synthesis SeNP was determined by XRD technique (Figure 3A). The depicted diffraction peaks at 2θ of 23.5°, 29.7°, 41.4°, 45.4°, and 51.7° were assigned to X-ray lattice planes (100), (101), (110), (111), and (201), respectively; the lattice constants were a= 4.365 Å, b=4.365 Å, and c= 4.953 Å. These data were in agreement with previous literature on biogenic synthesis of selenium nano-elements [4,19] and were confirmed with the reported standard in International Center for Diffraction Data (ICDD) card no. 06-0362. The size of the nanoparticles was determined using the full width at half maximum (FWHM = 0.229) for the lattice plane (101) through Scherrer's formula and found to be 37.55 nm. The unassigned diffraction peaks could be due to the secondary metabolites present in the aqueous extract of the plant [9]. The crystalline nature of MPM-SeNPs depicted herein was in accordance with reported biosynthesized nanoparticles using *Ceropegia bulbosa* [4], *Psidium guajava* [9], fenugreek [33], *Vitis vinifera* [39], and bee propolis [40] extracts. Furthermore, the presence of elemental selenium in biosynthesized nanoparticles was depicted with EDX analysis (Figure 3B); it revealed three absorption peaks, a small signal at 1.37 keV and two principal signals at 11.22 keV and 12.49 keV corresponding to L_α, K_α, and K_β families of X-rays specific for Se-element respectively, a finding that was in accordance with previous observation on SeNPs synthesized using fructose as reducing agent [41]. The analysis indicated that Se-element constituted 73.2% of the sample, K (10.8%), S (7.8%), Ca (5.4%), and P (1.1%), among others. The presence of absorption peaks corresponding to minerals was previously depicted in the EDX of a SeNPs synthesized by *M. oleifera* [42]; the presence of a peak for sulfur highlighted the role of protein; peaks for potassium, phosphorus, and calcium might attribute the high mineral content of *M. peregrina* extract, which all indicate their bounding to the surface of the nanoparticle and their role in stabilization as well as bio-reduction processes.

The SEM indicated that the biosynthesized MPM-SeNPs were agglomerated spheres of smooth surfaces with a diameter range of 80-150 nm (Figure 3C). Agglomeration of the spherical nanoparticles might be attributed to the functional groups (from the *M. peregrina* aqueous leave extract) decorating the particles' surfaces 38]. Consistent with our findings, SeNPs synthesized using *Zingiber officinale* fruit extract [7], fenugreek seed extract [33], *Allium Sativum* extract [43], and *Lycium barbarum* leave extract [44] were with average sizes of 100-150 nm, 50-150 nm, 40-110 nm, and 83-160 nm, respectively. However, the hydrodynamic size distribution and stability of the MPM-SeNPs were determined through DLS

and measuring zeta potential. The DLS pattern displayed two broad peaks (Figure 3D), indicating polydisperse in the size distribution of the nanoparticles, showing a mean hydrodynamic size 311.7±2.6 nm (Z-average) with a polydispersity index (PDI) of 0.34. A similar finding was recorded by SeNPs synthesized using *Petroselinum crispum* (parsley) with an average size around 400 nm [45]. Furthermore, the recorded zeta potential was at a maximum value of -60.8±2.6 mV, indicating stable dispersion in solution without aggregation; the high negative charge value on the nanoparticle's surfaces causes stability due to increased repulsions between the particles [5,6]. Such negative charged potential might be referred to as the reducing agents (e.g., phenolic compounds) [10], the side chain of some amino acid residues, and carboxylated polysaccharides [46]. The difference in the size distribution between SEM measurements and DLS is that the SEM measures the core nanoparticle's size. In contrast, DLS measures the hydrodynamic solvent coating (film) molecules around the SeNPs [10,39].

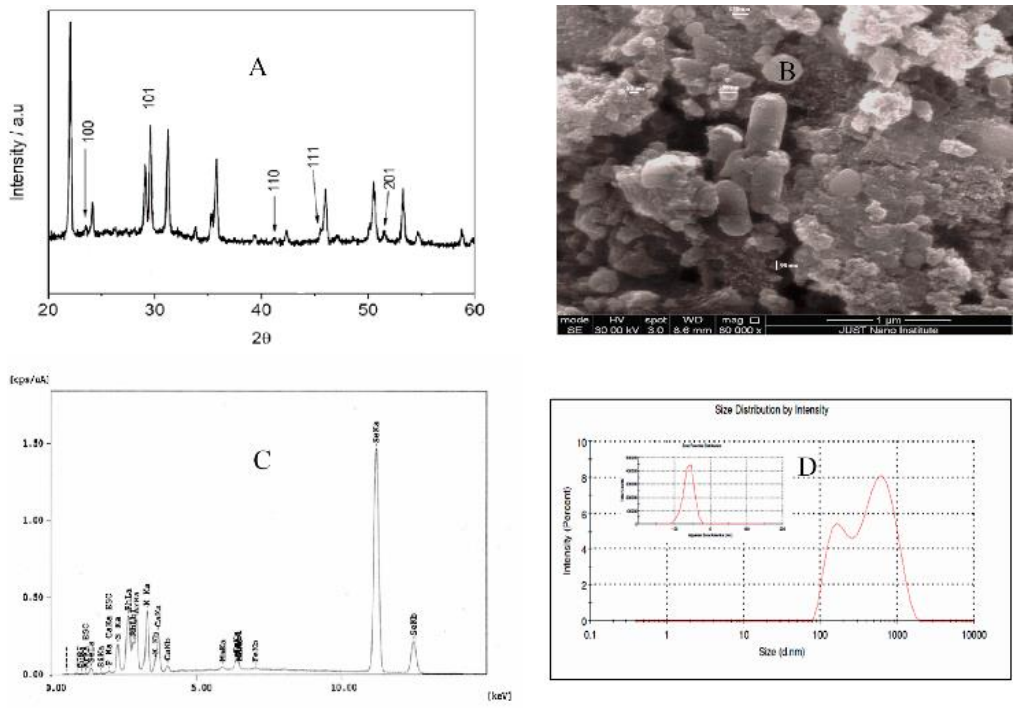

Figure 3. Characterization of phyto-synthesized MPM-SENPs. (**A**) XRD pattern reveals the crystalline structure of the nanoparticles, (**B**) SEM micrograph showing the shape and size of the nanoparticles at a magnification of 80 000X, (**C**) EDX pattern of the nanoparticles revealing its selenium composition, and (**D**) DLS pattern showing the hydrodynamic size of the nanoparticle and its zeta potential (inset).

3.3. Biological activities of MPM-SeNPs.

The synthesized nanoparticles revealed antibacterial activity against Gram-positive bacteria with inhibition zones ranging 12-19 mm in agar diffusion test and MIC values of 20-50 µg/mL (Table 1); Gram-negative bacteria were resistant to applied SeNPs; plant aqueous extract and Na_2SeO_3 were inactive against tested bacterial strains. In contrast, the positive control (streptomycin) exhibited a broad antibacterial activity against both types of bacterial test strains with significant MIC values of 0.8-3.2 µg/mL compared to the MPM-SeNPs ($p< 0.05$). The current finding reemphasizes the role SeNPs might have in counteracting the escalation in bacterial resistance to antibiotics and mitigating the morbidity and mortality rate due to infectious diseases, especially those due to food poisoning.

The susceptibility of Gram-positive bacteria over Gram-negative ones to tested nanoparticles was reported previously by several authors [7,10,40]. It was proposed that SeNPs

exert their antibacterial activity either through interacting with the peptidoglycan [9], leading to disturbing of the cell wall, interfering and disturbing the cell membrane by interacting with and deactivating membrane proteins, or causing cell death via oxidative stress-induced nucleic acid and protein damage [7,10]. Intriguingly, the presence of negative charges on the MPM-SeNPs' surfaces might cause electrostatic repulsion toward lipopolysaccharide moiety of the Gram-negative bacteria cell wall, which render them less susceptible than Gram-positive to tested SeNPs [10,47]; the presence of less negative net charge on the surface of Gram-positive bacteria facilitates the deposition of the SeNPs on bacterial membrane leading to the adverse effect on their growth and survival [48].

Table 1. Antibacterial activity of MPM-SeNPs (20 µg/disk) and streptomycin (10 µg/disk) against tested bacterial strains.

Bacterial strain	Zone of inhibition [mm ± SD]		MIC (µg/mL)	
	MPM-SeNPs	Streptomycin	MPM-SeNPs	Streptomycin
Gram-positive				
B. subtilis	18.7± 1.2	25.7± 1.2	20s	0.8c*
B. cereus	14.7± 0.6	22.3± 1.2	50s	0.8c*
S. aureus	12.3± 1.5	17.7± 0.6	50s	1.6s*
Gram-negative				
E. coli	NA	11.7± 0.6	>100	3.2s*
P. aeruginosa	NA	12.3± 0.7	>100	3.2s*

NA: not active at tested concentration c: bacteriocidic s: biostatic. *Statistically significant MIC-value compared to tested nanoparticles (p<0.05).

Evaluation of the antioxidant potential of biosynthesized SeNPs compared to that of the aqueous plant extract and Na_2SeO_3 indicated the superior radical neutralizing activity of the nanoparticles in both DPPH and ABTS assays. The antioxidant activities of tested samples were concentration-dependent and the concentrations required to scavenge 50% of DPPH radicals (IC_{50}) were 23.6±0.2 µg/mL (6.4±0.05 µg SeNPs/µg Trolox), 33.8.6±0.7 µg/mL (9.1±0.2 µg plant extract/µg Trolox), and 44.2±0.5 µg/mL (11.9± 0.1 µg Na_2SeO_3/µg Trolox). Meanwhile, the IC_{50} values for ABTS were 25.6±1.7 µg/mL (13.5±0.9 µg SeNPs/µg Trolox), 50.7±0.5 µg/mL (26.7±0.9 µg plant extract/µg Trolox), and 62.2±1 µg/mL (32.7±0.5 µg Na_2SeO_3/µg Trolox) (Table 2). Remarkably, there was a high correlation between the results in DPPH assay and that in ABTS method (r= 0.9) with the significant scavenging effect of the biosynthesized nanoparticle over the plant extract or the selenite precursor ($p< 0.05$) in both experiments. This high correlation between the two systems indicated that the functional groups on the surface of the nanoparticles are responsible for the inducing ability of these nanoparticles in neutralizing generated radicals in hydrophobic and hydrophilic protocols, especially the phenolic constituents.

Our results on the MPM-SeNPs antioxidant activity were consistent with the reported scavenging activity of phyto-synthesized SeNPs as primary antioxidant agents [10,38]. SeNPs synthesized using leave extract of *Emblica officinalis* revealed antioxidant activity with effective doses (EC_{50}) 18.84±1.02 µg/mL and 15.67±1.41 µg/mL in ABTS and DPPH assays, respectively [10]; a dose comparable with our findings. All previous reports highlighted that such activity is correlated not just to the size of nanoparticles but also to the functional groups from the phyto-extracts that were responsible for reducing the selenite precursor and capping the formed nanoparticles [7]; an observation that underlines the superior scavenging activity of the SeNPs decorated with phytochemical moieties over the plant extract *per se*.

Table 2. Antioxidants and activities of MPM-SENPs, plant aqueous extract, and sodium selenite in DPPH and ABTS assays.

Concentration of Sample µg/mL	% Inhibition ± SD					IC_{50} ± SD µg/mL
	5	10	25	50	100	
DPPH						
Plant extract	16.4±0.1	24.6±0.7	38.3±0.3	65.3±0.8	69.9±1.1	**33.8 ±0.7**
Na_2SeO_3	6.3±0.03	18.9±0.1	35.3±0.1	53.1±0.1	71.5±0.9	**44.2±0.5**
MPM-SeNPs	8.9±0.01	20.5±0.02	52.6±0.2	75.7±0.9	90.6±0.6	**23.6±0.2***
ABTS						
Plant extract	6.9±0.1	14.1±0.1	26.7±0.4	41.4±0.7	76.2±1.4	**50.7±0.5**
Na_2SeO_3	11.1±0.2	13.5±0.1	26.3±0.3	29.4±0.3	72.4±0.9	**62.2±1**
MPM-SeNPs	16.7±0.6	31.4±0.4	45.8±0.3	63.9±1.2	81.2±1.4	**25.6±1.7***

Trolox IC_{50} (µg/mL): DPPH 3.7 ± 0.3, ABTS 1.9 ± 0.2. Asterisk indicated statistically significant IC_{50} values between tested samples in the same test system ($p<0.05$).

The anti-proliferative activity of plant extract, Na_2SeO_3, and MPM-SeNPs was assessed against normal dermal fibroblast and breast adenocarcinoma cell lines. The plant extract was non-toxic to the normal cell line and had no antitumor potential up to 200 µg/mL. However, the phyto-synthesized SeNPs were less toxic than the sodium selenite precursor to normal cell line with IC_{50} values of 129.4±4.4 µg/mL compared to 1.7±0.1 µg/mL, respectively; Na_2SeO_3 exhibited pronounced cytotoxicity to fibroblast cells at concentrations starting from 1 µg/mL (Table 3). Similarly, surface fabrication of SeNPs with phytochemical moieties reduce it toxicity over Na_2SeO_3 against MDA-MB-231 breast cancer (IC_{50} 71.4±3.4 µg/mL vs. 2.82±0.2 µg/mL, respectively); though the MPM-SeNPs exerts marked anticancer activity starting from 10 µg/mL compared to over 50 µg/mL in case of the normal fibroblast cell line. (Table 3) revealed that MPM-SeNPs inhibited proliferation of breast cancer cell lines with IC_{50} of 71.4±3.4 µg/mL, a concentration that was non-toxic to the normal fibroblast cells, indicating its biocompatibility. Furthermore, the nanoparticles were 14 times more selective than the positive control (doxorubicin) in inhibiting MDA-MB-231 breast cancer cells proliferation; SI of MPM-SeNPs was 1.81 compared to 0.128 that of doxorubicin. Intriguingly, there was no dramatic decrease in the cell viability with an increase in tested nanoparticle concentrations between each subsequent dose; it might highlight the biostatic effect of MPM-SeNPs on the tested breast cell line with proposed apoptotic rather than necrotic effect.

In accordance with the current results, biosynthesized *C. bulbosa* mediated SeNPs showed anti-proliferative activity at IC_{50} 34 µg/mL against MDA-MB-231 breast cancer cells without affecting the viability of normal HBL-100 breast cells [4], and SeNPs synthesized using *E. offcinalis* leaves extract exhibited anti-mouse neuroblastoma N2a cell line activity at IC_{50} 14.01±1.88 µg/mL compared to 127.28±3.73 µg/mL for Na_2SeO_3 [10]. Furthermore, capping off the nanoparticles might enhance their uptake by endocytosis accumulation in cancer cells which consequently might lead to induce ROS production, disruption of mitochondrial membrane potential, and activation of mitochondrial-mediated apoptotic pathway through caspase 3/8 activation, and cellular growth arrest in G2/M phase [1]. Worth noting, the lack of plant extract to proliferative inhibition effect against MDA-MB-231 breast cancer cell line indicated that the anticancer activity of MPM-SeNPs was planting constituent independent, and it could be presumed that the nano-element itself played a key role in the antitumor activity [34].

Table 3. Anti-proliferative activity of MPM-SENPs, plant aqueous extract, and sodium selenite against normal fibroblast and MDA-MB-231 cell lines.

	% Inhibition in cell proliferation					
	Fibroblast			MDA-MB-231		
Concentration µg/mL	Plant extract	Na_2SeO_3	MPM-SeNPs	Plant extract	Na_2SeO_3	MPM-SeNPs
1	Nt	32.4±0.5	-	Nt	37±2.3	-
2	Nt	55±3.7	-	Nt	49.1±4.1	-
5	Nt	76.2±8.1	-	Nt	68.1±3.6	24.7±0.1
10	-	93.7±9.7	-	-	78.6±1.3	30.4±4.2
25	-	Nt	-	-	Nt	33.6±1.3
50	-	Nt	16.1±0.9	-	Nt	41.8±1.5
100	-	Nt	33.8±1	-	Nt	59.4±2.1
200	-	Nt	70.9±1.6	-	Nt	61.3±0.7
IC_{50} (µg/mL)	**> 200**	**1.7±0.1***	**129.4±4.4****	**> 200**	**2.82±0.2**	**71.4±3.4****

Doxorubicin IC_{50} (µg/mL): Fibroblast: 0.32±0.02, MDA-MB-231: 2.5±0.1, nt: not tested, -: inhibition < 10%. Asterisks indicated statistically significant differences in IC_{50} values (µg/mL) of tested samples to positive control against the same cell line (* $0.01<p<0.05$, ** $p<0.01$).

4. Conclusions

The current study represented the first work that appraises the bio-reductive synthesis of SeNPs using *M. peregrina* leaves extract. Likewise, it highlighted the antibacterial, antioxidant, and anti-breast cancer activity with compatibility in normal cells. Surface phyto-decoration of the SeNPs is much more acceptable than chemically, or microorganism-mediated synthesized nanoparticles with improved stability, cellular uptake, and bioactivity. Therefore, they could potentially substitute synthetic chemotherapeutic drugs and be used as a natural agent in the food and pharmaceutical industries.

Funding

This research received no external funding.

Acknowledgments

The authors would like to acknowledge the Deanship of the Scientific Research/University of Jordan for the financial support. Appreciation is due to Dr. Qosay Al-Balas, Prof. Anas Al-Nabulsi, and Mrs. Sawsan Mutlaq from the Department of nutrition/Jordan University of Science and Technology for carrying out XRD, SEM, and DLS analysis. Prof. Mohammed Al-Anbar and Prof. Ayman Al-Qtaitat, Department of Chemistry and Department of Medicine-Mutah University, are acknowledged for performing the FT-IR and EDX analyses.

Conflicts of Interest

The authors declare no conflict of interest.

References

1. Khurana, A.; Tekula, S.; Saifi, M.A.; Venkates, P.; Godugu, C. Therapeutic applications of selenium nanoparticles. *Biomedicine and Pharmacotherapy* **2019**, *111*, 802-812, https://doi.org/10.1016/j.biopha.2018.12.146.
2. Ikram, M.; Javed, B.; Raja, N.I.; Mashwani, ZU. Biomedical potential of plant-based selenium nanoparticles: a comprehensive review on therapeutic and mechanistic aspects. *International Journal of Nanomedicine* **2021**, *16*, 249-268, https://doi.org/10.2147/IJN.S295053.

3. Menon, S.; Shanmugam, V. Cytotoxicity analysis of biosynthesized selenium nanoparticles towards A549 lung cancer cell line. *Journal of Inorganic and Organometallic Polymers and Materials* **2020**, *30*, 1852-1864, https://doi.org/10.1007/s10904-019-01409-4.
4. Cittrarasu, V.; Kaliannan, D.; Dharman, K.; Maluventhen, V.; Easwaran, M.; Liu, W.C. Green synthesis of selenium nanoparticles mediated from *Ceropegia bulbosa* Roxb extract and its cytotoxicity, antimicrobial, mosquitocidal and photocatalytic activities. *Scientific Reports* **2021**, *11*, 1-5, https://doi.org/10.1038/s41598-020-80327-9.
5. Joshi, S.M.; De Britto, S.; Jogaiah, S. Mycogenic selenium nanoparticles as potential new generation broad spectrum antifungal molecules. *Biomolecules* **2019**, *9*, 419, https://doi.org/10.3390/biom9090419.
6. Cong, W.; Bai, R.; Li, Y.F.; Wang, L.; Chen, C. Selenium nanoparticles as an efficient nanomedicine for the therapy of Huntington's disease. *ACS Applied Materials and Interfaces* **2019**, *11*, 34725-34735, https://doi.org/10.1021/acsami.9b12319.
7. Menon, S.; Agarwal, H.; Shanmugam, V.K. Efficacy of biogenic selenium nanoparticles from an extract of ginger towards evaluation on antimicrobial and antioxidant activities. *Colloid and Interface Science Communications* **2019**, *29*, 1-8, https://doi.org/10.1016/j.colcom.2018.12.004.
8. Liu, F.; Liu, H.; Liu, R.; Xiao, C.; Duan, X.; McClements, D.J. Delivery of sesamol using polyethylene-glycol-functionalized selenium nanoparticles in human liver cells in culture. *Journal of Agricultural and Food Chemistry* **2019**, *67*, 2991-2998, https://doi.org/10.1021/acs.jafc.8b06924.
9. Alam, H.; Khatoon, N.; Raza, M.; Ghosh, P.C.; Sardar, M. Synthesis and characterization of nano selenium using plant biomolecules and their potential applications. *BioNanoScience* **2019**, *9*, 96-104, https://doi.org/10.1007/s12668-018-0569-5.
10. Gunti, L.; Dass, R.S.; Kalagatur, N.K. Phytofabrication of selenium nanoparticles from *Emblica officinalis* fruit extract and exploring its biopotential applications: antioxidant, antimicrobial, and biocompatibility. *Frontiers in Microbiology* **2019**, *10*, 931, https://doi.org/10.3389/fmicb.2019.00931.
11. El-Seedi, H.R.; El-Shabasy, R.M.; Khalifa, S.A.; Saeed, A.; Shah, A.; Shah, R. Metal nanoparticles fabricated by green chemistry using natural extracts: biosynthesis, mechanisms, and applications. *RSC Advances* **2019,** *9*, 24539-24559, https://doi.org/10.1039/C9RA02225B.
12. Dhakad, A.K.; Ikram, M.; Sharma, S.; Khan, S.; Pandey, V.V.; Singh, A. Biological, nutritional, and therapeutic significance of *Moringa oleifera* Lam. *Phytotherapy Research* **2019**, *33*, 2870-2903, https://doi.org/10.1002/ptr.6475.
13. Bindhu, M.R.; Umadevi, M.; Esmail, G.A.; Al-Dhabi, N.A.; Arasu, M.V. Green synthesis and characterization of silver nanoparticles from *Moringa oleifera* flower and assessment of antimicrobial and sensing properties. *Journal of Photochemistry and Photobiology B: Biology* **2020**, *205*, 111836, https://doi.org/10.1016/j.jphotobiol.2020.111836.
14. Belliraj, T.S.; Nanda, A.; Ragunathan, R. In-vitro hepatoprotective activity of *Moringa oleifera* mediated synthesis of gold nanoparticles. *Journal of Chemical and Pharmaceutical Research* **2015**, *7*, 781-788, https://www.jocpr.com/articles/invitro-hepatoprotective-activity-of-moringa-oleifera-mediatedsynthesis-of-gold-nanoparticles.pdf.
15. Khor, K.Z.; Joseph, J.; Shamsuddin, F.; Lim, V.; Moses, E.J.; Samad, N.A. The cytotoxic effects of *moringa oleifera* leaf extract and silver nanoparticles on human kasumi-1 cells. *International Journal of Nanomedicine* **2020**, *15*, 5661-5670, https://doi.org/10.2147/IJN.S244834.
16. Irfan, M.; Munir, H.; Ismail, H. *Moringa oleifera* gum-based silver and zinc oxide nanoparticles: green synthesis, characterization and their antibacterial potential against MRSA. *Biomaterials Research* **2021**, *25*, 1-8, https://doi.org/10.1186/s40824-021-00219-5.
17. Senthilkumar A, Karuvantevida N, Rastrelli L, Kurup SS, Cheruth AJ. Traditional uses, pharmacological efficacy, and phytochemistry of *Moringa peregrina* (Forssk.) Fiori. —a review. *Frontiers in Pharmacology* **2018**, *9*, 465, https://doi.org/10.3389/fphar.2018.00465.
18. Codesido, S.; Guillarme, D.; Fekete, S. Algorithms to optimize multi-column chromatographic separations of proteins. *Journal of Chromatography A* **2021**, *1637*, 461838, https://doi.org/10.1016/j.chroma.2020.461838.
19. Srivastava, P.; Kowshik, M. Anti-neoplastic selenium nanoparticles from *Idiomarina* sp. PR58-8. *Enzyme and Microbial Technology* **2016**, *95*, 192-200, https://doi.org/10.1016/j.enzmictec.2016.08.002.
20. Al-Zereini WA. Bioactive crude extracts from four bacterial isolates of marine sediments from Red Sea, Gulf of Aqaba, Jordan. *Jordan Journal of Biological Sciences* **2014**, *7*, 133-137, https://jjbs.hu.edu.jo/files/v7n2/Paper%20Number%208%5B1%5D.pdf.

21. Al-Qaralleh, O.S.; Al-Zereini, W.A.; Al-Mustafa, A.H. Antibacterial, antioxidant and neuroprotective activities of crude extract from the endophytic fungus *Fusarium* sp. isolate OQ-Fus-2-F from *Euphorbia* sp. plant. *Journal of Pharmacy and Pharmacognosy Research* **2021**, *9*, 755-765, https://jppres.com/jppres/pdf/vol9/jppres21.1077_9.6.755.pdf.
22. Al-Zereini, W.A. *Ononis natrix* and *Salvia verbenaca*: Two Jordanian medicinal plants with cytotoxic and antibacterial activities. *Journal of Herbs, Spices and Medicinal Plants* **2017**, *23*, 18-25, https://doi.org/10.1080/10496475.2016.1241200.
23. Shao, K.; Andrew, J. S. A Web-Based System for Bayesian Benchmark Dose Estimation. *Environmental Health Perspectives* **2018**, *126*, 1–14, https://doi.org/10.1289/EHP1289.
24. Amira, S.H.; Awatif, I.; Ismael, Mohamed, S.; Abbas, Hisham, A.; Abd El-Lateaf; Marwa, E. Comparative Characteristics Study of Moringa (*Moringa peregrina*), Terminalia (Terminalia Billerica) and Tiger nut (Cyperus esculentus) Oils. *Egyptian Journal of Chemistry* **2021**, *64*, 5241–5248, https://doi.org/10.21608/EJCHEM.2021.70105.3585.
25. Sulastri, E.; Zubair, M.S.; Anas, N.I.; Abidin, S.; Hardani, R.; Yulianti, R. Total phenolic, total flavonoid, quercetin content and antioxidant activity of standardized extract of *Moringa oleifera* leaf from regions with different elevation. *Pharmacognosy Journal* **2018,** *10*, 104-108, https://doi.org/10.5530/pj.2018.6s.20.
26. Hamed, M.M.; Mohamed, M.A.; Ahmed, W.S. Chemical constituents, in vitro antioxidant activity, oral acute toxicity and LD_{50} determination of *Moringa oleifera* leaves. *International Journal of Pharmacy and Pharmaceutical Sciences* **2017**, *9*, 240-247, https://doi.org/10.22159/ijpps.2017v9i5.17834.
27. El-Awady, M.A.; Hassan, M.M.; El-Sayed, S.A.; Gaber, A. Comparison of the antioxidant activities, phenolic and flavonoids contents of the leaves-crud extracts of *Moringa peregrina* and *Moringa oleifera*. *International Journal of Biosciences* **2016**, *8*, 55-62, http://dx.doi.org/10.12692/ijb/8.1.55-62.
28. Dehshahri, S.H.; Wink, M.; Afsharypuor, S.; Asghari, G.; Mohagheghzadeh, A. Antioxidant activity of methanolic leaf extract of *Moringa peregrina* (Forssk.) Fiori. *Research in Pharmaceutical Sciences* **2012**, *7*, 111-118, https://www.ncbi.nlm.nih.gov/pmc/articles/PMC3501899/pdf/JRPS-7-111.pdf.
29. Abo El-Fadl, S.; Osman, A.; Al-Zohairy, A.M.; Dahab, A.A.; Abo El Kheir, Z.A. Assessment of phenolic, flavonoid content, antioxidant potential and HPLC profile of three *Moringa* species leaf extracts. *Scientific Journal of Flowers and Ornamental Plants* **2020**, *7*, 53-70, https://doi.org/10.21608/sjfop.2020.91397.
30. Sreelatha, S.; Padma, P.R. Antioxidant activity and total phenolic content of *Moringa oleifera* leaves in two stages of maturity. *Plant Foods for Human Nutrition*. **2009**, *64*, 303-311, https://doi.org/10.1007/s11130-009-0141-0.
31. Hossain, M. A.; Disha, N. K.; Shourove, J. H.; Dey, P. Determination of Antioxidant Activity and Total Tannin from Drumstick (*Moringa oleifera* Lam) Leaves Using Different Solvent Extraction Methods. *Turkish Journal of Agriculture* **2020**, *8*, 2749-2755, https://doi.org/10.24925/turjaf.v8i12.2749-2755.4038.
32. Jan, R.; Asaf, S.; Numan, M.; Lubna; Kim, K.-M. Plant Secondary Metabolite Biosynthesis and Transcriptional Regulation in Response to Biotic and Abiotic Stress Conditions. *Agronomy* **2021**, *11*, 968, https://doi.org/10.3390/agronomy11050968.
33. Ramamurthy, C.H.; Sampath, K.S.; Arunkumar, P.; Kumar, M.S.; Sujatha, V.; Premkumar, K. Green synthesis and characterization of selenium nanoparticles and its augmented cytotoxicity with doxorubicin on cancer cells. *Bioprocess and Biosystems Engineering* **2013**, *36*, 1131-1139, https://doi.org/10.1007/s00449-012-0867-1.
34. Cui, D.; Liang. T.; Sun, L.; Meng, L.; Yang, C.; Wang, L. Green synthesis of selenium nanoparticles with extract of hawthorn fruit induced HepG2 cells apoptosis. *Pharmaceutical Biology* **2018**, *56*, 528, https://doi.org/10.1080/13880209.2018.1510974.
35. Husen, A.; Siddiqi, K.S. Plants and microbes assisted selenium nanoparticles: characterization and application. *Journal of Nanobiotechnology* **2014**, *12*, https://doi.org/10.1186/s12951-014-0028-6.
36. Kora, A.J.; Rastogi, L. Biomimetic synthesis of selenium nanoparticles by *Pseudomonas aeruginosa* ATCC 27853: an approach for conversion of selenite. *Journal of Environmental Management* **2016**, *181*, 231-236, https://doi.org/10.1016/j.jenvman.2016.06.029.
37. Wang, Y.; Shu, X.; Zhou, Q.; Fan, T.; Wang, T.; Chen, X. Selenite reduction and the biogenesis of selenium nanoparticles by *Alcaligenes faecalis* Se03 isolated from the gut of *Monochamus alternatus* (Coleoptera: Cerambycidae). *International Journal of Molecular Sciences* **2018**, *19*, 2799, https://doi.org/10.3390/ijms19092799.

38. Alagesan, V.; Venugopal, S. Green synthesis of selenium nanoparticle using leaves extract of *Withania somnifera* and its biological applications and photocatalytic activities. *Bionanoscience* **2019**, *9*, 105-116, https://doi.org/10.1007/s12668-018-0566-8.
39. Sharma, G.; Sharma, A.R.; Bhavesh, R.; Park, J.; Ganbold, B.; Nam, J.S. Biomolecule-mediated synthesis of selenium nanoparticles using dried *Vitis vinifera* (raisin) extract. *Molecules* **2014**, *19*, 2761-2770, https://doi.org/10.3390/molecules19032761.
40. Shubharani, R.; Mahesh, M.; Yogananda, Murthy, V. Biosynthesis and characterization, antioxidant and antimicrobial activities of selenium nanoparticles from ethanol extract of Bee Propolis. *Journal of Nanomedicine and Nanotechnology* **2019**, 10, https://doi.org/10.4172/2157-7439.1000522.
41. Vieira, A.P.; Stein, E.M.; Andreguetti, D.X.; Cebrián-Torrejón, G.; Doménech-Carbó, A.; Colepicolo, P. Sweet Chemistry: a green way for obtaining selenium nanoparticles active against cancer cells. *Journal of the Brazilian Chemical Society* **2017**, *28*, 2021-2027, https://doi.org/10.21577/0103-5053.20170025.
42. Hassanien, R.; Abed-Elmageed, A.A.; Husein, D.Z. Eco-friendly approach to synthesize selenium nanoparticles: photocatalytic degradation of sunset yellow azo dye and anticancer activity. *ChemistrySelect* **2019**, *4*, 9018-9026, https://doi.org/10.1002/slct.201901267.
43. Anu, K.; Devanesan, S.; Prasanth, R.; AlSalhi, M.S.; Ajithkumar, S.; Singaravelu, G. Biogenesis of selenium nanoparticles and their anti-leukemia activity. *Journal of King Saud University-Science* **2020**, *32*, 2520-2526, https://doi.org/10.1016/j.jksus.2020.04.018.
44. Zhang, W.; Zhang, J.; Ding, D.; Zhang, L.; Muehlmann, L.A.; Deng, S.E. Synthesis and antioxidant properties of *Lycium barbarum* polysaccharides capped selenium nanoparticles using tea extract. *Artificial Cells, Nanomedicine, and Biotechnology* **2018**, *46*, 1463-1470, https://doi.org/10.1080/21691401.2017.1373657.
45. Alipour, S.; Sara, K.; Mohammad, H. M.; Zahra, S.; Ali D. Green Synthesis of Selenium Nanoparticles by *Cyanobacterium Spirulina* Platensis (Abdf2224): Cultivation Condition Quality Controls. *BioMed Research International* **2021**, https://doi.org/10.1155/2021/6635297.
46. Pyrzynska, K.; Sentkowska, A. Biosynthesis of selenium nanoparticles using plant extracts. *Journal of Nanostructure in Chemistry* **2021**, *28*, 1-4, https://doi.org/10.1007/s40097-021-00435-4.
47. Truong, L, B.; David, M.; Ebrahim. M. Selenium Nanomaterials to Combat Antimicrobial Resistance. *Molecules* **2021**, *26*, 3611, https://doi.org/10.3390/molecules26123611.
48. Vahdati, M.; Moghadam, T.T. Synthesis and characterization of selenium nanoparticles-lysozyme nanohybrid system with synergistic antibacterial properties. *Scientific Reports* **2020**, *10*, https://doi.org/10.1038/s41598-019-57333-7.